Distinguishing between Two-State and Three-State Models for Ubiquitin Folding†

Bryan A. Krantz and Tobin R. Sosnick*

Department of Biochemistry and Molecular Biology, University of Chicago, 920 East 58th Street, Chicago, Illinois 60637

Received April 10, 2000; Revised Manuscript Received July 26, 2000

ABSTRACT: Conflicting results exist regarding whether the folding of mammalian ubiquitin at 25 °C is a simple, two-state kinetic process or a more complex, three-state process with a defined kinetic intermediate. We have measured folding rate constants up to about 1000 s^{-1} using conventional rapid mixing methods in single-jump, double-jump, and continuous-flow modes. The linear dependence of folding rates on denaturant concentration and the lack of an unaccounted "burst-phase" change for the fluorescence signal indicate that a two-state folding model is adequate to describe the folding pathway. This behavior also is seen for folding in the presence of the stabilizing additives 0.23 M sodium sulfate and 1 M sodium chloride. These results stress the need for caution in interpreting deviations from ideal two-state "chevron" behavior when folding is heterogeneous or folding rate constants are near the detection limit.

Despite the high dimensionality of the reaction surface, many small globular proteins fold in a kinetically two-state manner: U ↔ N (*1*). This observation is powerful, because it places strong constraints on any relevant folding model. For example, two-state behavior mandates that any intermediate more stable than the denatured state must exist on the native side of the rate-limiting barrier under refolding conditions (Figure 1a). Based upon this and other observations, we and others have proposed that the folding of small globular proteins (<∼100 amino acids) is a nucleation process (*2*−*6*) with a limiting step that is relatively early in the folding process (*2, 4*−*6*).

Although most small proteins fold in a two-state manner, a few systems are reported to fold in a three-state fashion with a marginally stable intermediate forming on the denatured side of the major kinetic barrier (*1*)(Figure 1b): $U \xrightarrow{\text{fast}} I \xrightarrow{\text{slow}} N$. The focus of the present study is one of the most frequently cited examples of a three-state system, mammalian ubiquitin (Ub),[1] a 76 amino acid α/β protein (*7*−*9*). For the fluorescent F45W mutant at 25 °C, Roder and co-workers have proposed that a stable intermediate is formed in less than a millisecond at low concentrations of denaturant (*8, 9*). They observed that the standard free energy of activation "rolls-over" and plateaus at a maximal folding rate constant at low denaturant concentration, and the chevron-style plot (*10*) deviates from the perfect "V" shape typical of two-state folding systems. Also, a significant fraction of the fluorescence signal is lost in the millisecond instrumental dead-time, τ_d, at low denaturant concentrations. This unaccounted signal, or "burst-phase" amplitude, exhibits a sharp dependence on denaturant concentration indicative of a cooperative folding process from the U state to a highly compact I state.

On the other hand, a variety of other results for Ub are consistent with a two-state folding behavior. Hydrogen exchange (HX) labeling studies (*7, 8, 11*) failed to observe amide H-bond formation in the first few milliseconds of refolding. In fact, studies by Gladwin and Evans at 20 °C indicated that all the amide protons exchange with protection factors near unity, indicating that the backbone is as exposed as in random coil polypeptide (*11*). Likewise, their stopped-flow far-UV circular dichroism studies failed to observe any burst phase intermediate (*11*). These data argue against the proposed kinetic intermediate (*8, 9*) because any such species having the majority of the total surface buried in the U → N reaction should have had some secondary structure and HX slowing.

Furthermore, Ub folds in a two-state manner at lower temperatures, as seen at 8 °C (*8*) and at 10 °C (*12*), where folding rate constants are readily measurable with a conventional stopped-flow apparatus. In these studies, the folding rate constant remains linear over all denaturant concentrations, and the fluorescent signal is completely accounted for in the observed phase. Also, our D/H amide kinetic isotope studies suggest only minimal structure formation is formed prior to the transition state (*12*).

Last, submicrosecond temperature-induced refolding measurements by Gruebele and co-workers on cold-denatured ubiquitin show no evidence of an intermediate at 2 °C (after accounting for a solvent-dependent response of the unfolded state) (*13*). More complex kinetics are observed at 8 °C, but the reaction surface still is viewed as consistent with a two-state system. The very fast folding population represents a subfraction of the −8 °C, cold-denatured ensemble whose configuration is such that upon the nanosecond T-jump, these molecules reside on the native side of the rate-limiting barrier on the new +8 °C reaction surface.

Given these apparently conflicting results for such a well-studied protein and the importance of understanding the role of stable kinetic intermediates, we investigated whether Ub's

† This work was supported in part by NIH Grant GM55694 (T.R.S.), The Packard Foundation Interdisciplinary Science Program (T.R.S., P.Thiyagarajan, S. Berry, D. Lynn, S. Meredith), and National Cancer Institute Grant CA14599 to the University of Chicago Cancer Research Center.

* Corresponding author. Phone: (773)834-0657; Fax: (773)702-0439; E-mail: trsosnic@midway.uchicago.edu.

[1] Abbreviations: GdmCl, guanidinium chloride; HX, hydrogen exchange; τ_d, stopped-flow dead-time; Ub, ubiquitin.

10.1021/bi000792+ CCC: $19.00
Published on Web 08/25/2000

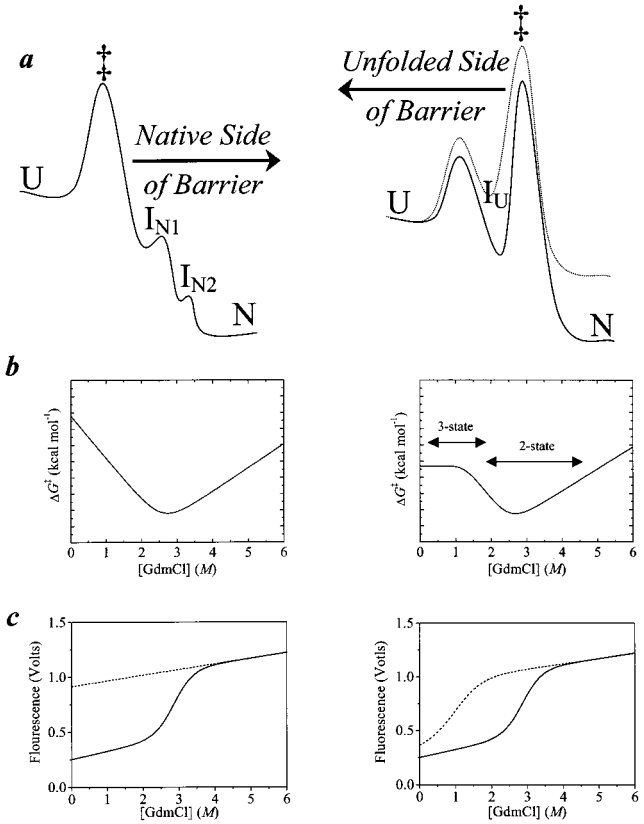

FIGURE 1: Folding behavior for model two-state (left) and three-state (right) systems. (a) Free energy diagrams. An intermediate, I, occurring prior to the rate-limiting step (denoted by ‡) is observed in refolding experiments when it is stable relative to the unfolded state. (b) Denaturant dependence of standard free energy of activation. The roll-over can be described as the three-state region of the chevron (solid line on right side) where the remainder of the chevron is predominantly two-state (dotted line on right side). The three-state plot shown assumes that the amount of surface buried in the I state is the same as in the transition state, as previously proposed for Ub (*9*). (c) Amplitudes of the observed signal. The final amplitude (solid line) represents the equilibrium values. In the three-state scenario at low denaturant concentrations, there is a significant loss of signal with a sharp sigmoidal dependence indicative of a cooperative U-to-I melting transition.

folding behavior is kinetically two- or three-state. Specifically, we examined whether a two-state model is adequate to account for the denaturant dependence of folding rate constants and the amplitude of the observed signal changes. We have found that a two-state model adequately describes the folding pathway of Ub under conditions where an intermediate reportedly existed (*8, 9*).

MATERIALS AND METHODS

Chemicals. Ultrapure guanidinium chloride (GdmCl) was purchased from ICN Biomedicals (Aurora, OH). All other chemicals were purchased from Fisher Scientific (Fair Lawn, NJ).

Protein. The wild-type expression vector, pRSUB, for human ubiquitin (Entrez gi576323, pdb 1UBI) was modified using the Stratagene Quick Change Mutagenesis Kit to create the F45W mutation. Expression and purification were carried out as described previously (*14*).

Equilibrium Measurements. Standard free energies of folding, $\Delta G°$, were determined from GdmCl denaturation profiles monitored by circular dichroism spectroscopy at 222 nm using a Jasco J-715 spectropolarimeter with a computer-interfaced titrator. Measurements were conducted with 2 nm resolution and a 1 cm path length cuvette. Peptide concentrations were 5 μM, and experiments were carried out in 20 mM sodium acetate.

Stopped-Flow Spectroscopy. Rapid mixing experiments used a Biologic SFM4 stopped-flow apparatus connected via a fiber optic cable to a PTI A101 arc lamp. Fluorescence spectroscopy used excitation and emission wavelengths of 280−290 and 300−400 nm, respectively. Fluorescence data were monitored with a Hamamatsu H5784 photomultiplier tube. Data were sampled every 50 μs with a matching RC filter. Temperature control of the sample syringes and the observation cuvette was maintained using a circulating water bath. Rate constants were determined using the Biologic Biokine software. The dead-time, τ_d, of the stopped-flow apparatus, using a 0.8 × 0.8 mm^2 square (FC/08) cuvette, was 1.3−1.7 ms depending upon syringe speed and dilution ratio. The dead-time was calibrated using a dye quenching reaction.

For the single-jump measurements, starting from the fully unfolded state (4−7 M GdmCl) or the folded state (1 M GdmCl), folding or refolding reactions were initiated by dilution to yield the desired denaturant concentration. Total volume per shot was 0.25 mL, except for dilutions greater than 1:8 where the total volume delivered was increased up to 0.5 mL This extra volume was required in order to ensure that the observed folding reaction was from a fresh protein solution that was uncontaminated by mixing with refolding buffer between shots. Failure to do so resulted in a minor, prefolded population and an accompanying change in the fluorescence signal, as determined by continuous-flow control experiments.

For the double-jump measurements, the native protein in 2 M GdmCl was mixed with 7.4 M GdmCl to a final concentration of 4.7 M GdmCl. After a 10 s delay (about 10 unfolding half-lives), the ~40 μL denatured protein solution contained in the aging loop was diluted with buffer to yield the final denaturant concentration. Continuous-flow measurements used the same protocol as the single-jump measurements, but the flow-speed was reduced to produce the desired dead-time [τ_d = (dead volume)/(flow-speed)].

Protein concentrations were 0.7−2.6 and 1.3 μM for the single-jump and double-jump measurements, respectively. Two to six time courses were averaged at each reaction condition.

Kinetic Analysis. The data were analyzed using the "chevron analysis" of the denaturant dependence of folding rate constants (*10*) where the standard free energy of folding, $\Delta G°$, along with the standard activation free energies for folding, $\Delta G_f^{\ddagger}$, and unfolding, $\Delta G_u^{\ddagger}$, are linearly dependent on denaturant concentration:

$$\Delta G°([\text{GdmHCl}]) = \Delta G_{\text{Equil}}^{H_2O} + m^{o}[\text{GdmHCl}] = -RT \ln (K_u) \quad (1a)$$

$$\Delta G_f^{\ddagger}([\text{GdmHCl}]) = -RT \ln k_f^{H_2O} - m_f[\text{GdmHCl}] + \text{constant} \quad (1b)$$

$$\Delta G_u^{\ddagger}([\text{GdmHCl}]) = -RT \ln k_u^{H_2O} - m_u[\text{GdmHCl}] + \text{constant} \quad (1c)$$

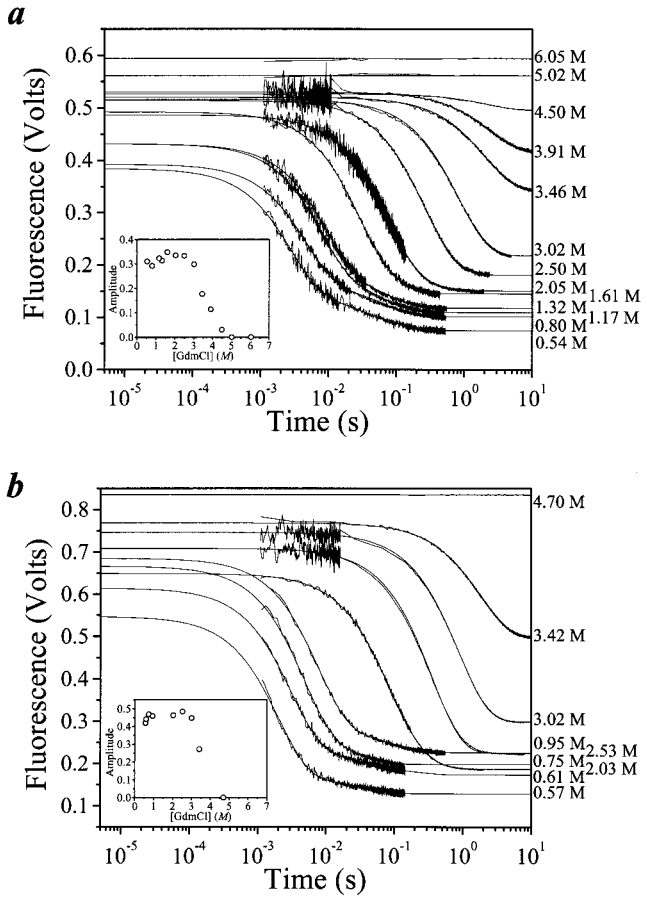

FIGURE 2: Denaturant dependence of folding at pH 5.0, 25 °C. Raw data traces in (a) single-jump refolding experiments and (b) double-jump refolding experiments which eliminate extraneous proline phases. The noncoincidence of the fully folded values largely represents the denaturant dependence of the native state (see Figure 3b). Inset: total amplitude change. In the two-state model, the change should be constant given that the slopes of the denaturant-dependent baselines of the denatured and native states are equivalent, as is the case (Figure 3b). The data, sampled every 50 μs, are binned into increasing longer time intervals which results in the decrease in the noise level.

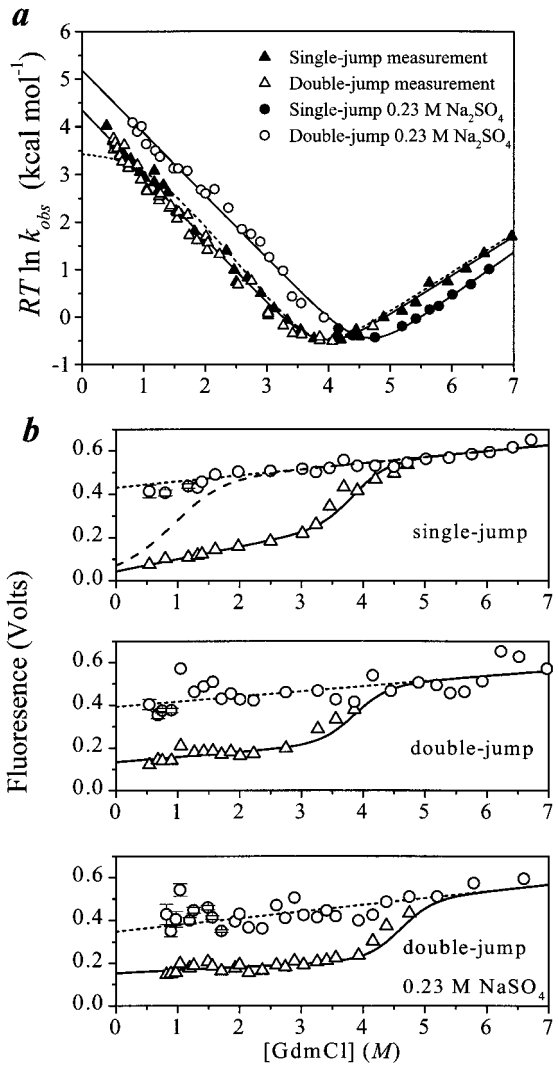

FIGURE 3: Denaturant dependence of folding at pH 5.0, 25 °C. (a) Folding activation energies for single- and double-jump protocols in the absence and presence of 0.23 M sodium sulfate. The dashed line is the fit to Ub F45W kinetic data reported previously (*9*). (b) The raw fluorescence signal (photomultiplier voltage) for single-jump and for double-jump measurements in the absence and presence of 0.23 M sodium sulfate. Amplitudes are defined by the raw fluorescence signals at the beginning (○) after extrapolation to $t = 0$ and end (△) of each refolding kinetic measurement. The solid line is fit to a two-state equilibrium denaturation profile using values from Table 1. The dashed line is a linear fit to the denaturant dependence of the unfolded state's fluorescence signal. The long dashed line in the top panel is the fit to the burst phase amplitudes from ref (*9*). Error bars at low denaturant concentrations represent the uncertainty of the extrapolated amplitude when the folding half-life is on the order of the instrumental dead-time.

where R is the gas constant, T is the temperature, and the dependence on denaturant concentration, the m-values, reports on the degree of surface area burial during the folding process. When equilibrium and kinetic folding reactions are effectively two-state and are limited by the same activation barrier, the equilibrium values for the standard free energy and surface burial can be calculated from kinetic measurements according to $\Delta G^\circ = \Delta G_f^\ddagger - \Delta G_u^\ddagger$ and $m^o = m_u - m_f$. Parameters were fit using a nonlinear least-squares algorithm implemented in the Microcal Origin software package.

RESULTS

Single-Jump Measurements. We performed stopped-flow fluorescence measurements in 20 mM sodium acetate, pH 5, 25 °C (Figure 2a). As observed in previous refolding studies of Ub at this condition (*8*, *9*), the fluorescence trace is largely, but not completely, monophasic, with the major phase representing the folding to the native state (*8*). As with certain other proteins including chymotrypsin inhibitor 2 (*15*) and src SH3 domain (*16*), the minor slow phases in Ub are predominantly associated with a population of slow folding molecules containing non-native cis proline isomers (native Ub has three trans prolines).

Our measured folding and unfolding activation free energies for the major phase are in very good agreement with the earlier studies (*8*, *9*) except that our folding values remain linear down to the lowest denaturant concentration measured (0.5 M GdmCl) and the resulting chevron plot has the ideal "V" shape typical of a two-state folding proteins (Figure 3a). Although the rate constants are approaching the limit of our stopped-flow apparatus, ~50% of the amplitude is observable for a rate constant of 500 s^{-1}. Additionally, the entire fluorescence signal is accounted for in the observed

Table 1: Thermodynamic and Kinetic Parameters for Ub Folding

experimental conditions	$-\Delta G_{equil}$ (kcal mol^{-1})	m^0_{equil} (kcal mol^{-1} M^{-1})	$-\Delta G_{kinetics}$ (kcal mol^{-1})	$RT \ln k_f^{H_2O}$ (kcal mol^{-1})[c]	$m^0_{kinetics}$ (kcal mol^{-1} M^{-1})	m_f (kcal mol^{-1} M^{-1})
25 °C[a]	8.19 ± 0.10	2.18 ± 0.02	8.40 ± 0.24	4.35 ± 0.04	2.17 ± 0.04	1.35 ± 0.02
25 °C/0.23 M sulfate[a]	9.50 ± 0.37	2.13 ± 0.09	10.2 ± 0.5	5.18 ± 0.06	2.23 ± 0.09	1.31 ± 0.03
5 °C/1.0 M NaCl[b]	8.42 ± 0.25	2.23 ± 0.06	8.20 ± 0.20	3.73 ± 0.03	2.18 ± 0.04	1.37 ± 0.02
15 °C/1.0 M NaCl[b]	8.71 ± 0.22	2.24 ± 0.05	9.28 ± 0.27	4.49 ± 0.03	2.24 ± 0.05	1.32 ± 0.02
25 °C/1.0 M NaCl[b]	9.39 ± 0.37	2.23 ± 0.09	9.70 ± 0.34	5.11 ± 0.03	2.28 ± 0.06	1.32 ± 0.02

[a] 20 mM sodium acetate, pH 5.0. [b] 20 mM sodium acetate, pH 4.5. [c] Extrapolated refolding activation energy in the absence of denaturant.

phase upon extrapolation to zero time (Figure 2a, inset, and Figure 3b). Neither of the two signatures of a folding intermediate, a saturation in the refolding rate constant and a burst phase amplitude, are observed at low denaturant concentrations. Also, the kinetic data interpreted in the context of a two-state model reproduce the equilibrium stability and surface area burial as determined from independent equilibrium denaturation measurements (Table 1).

It should be noted that an accurate determination of the fastest rate constants is difficult because they are near the limit of our apparatus and folding is heterogeneous, in large part due to proline isomerization. The fluorescence traces are multiphasic, and three to five exponential terms are required to fit the data over an extended time range. The second fastest phase accounts for up to ~20% of the amplitude, and its rate constant is within a factor of 5 of the fastest rate constant. The rate constants shown in Figure 3 are obtained using a biexponential fit over a limited time range at GdmCl concentrations below 2 M and monoexponential fits above 2 M.

The present combination of fast folding and heterogeneity can result in the fastest rate constants being underestimated. A portion of the fluorescence signal is unobservable due to the dead-time of the stopped-flow apparatus. As the folding rate constant increases, less of the major phase is observed and the proline-related phases contribute progressively more to the measured portion of the signal. These proline-related phases then may inadvertently be included in the fit to the fastest phase. Hence, as the rate of the fastest phase increases, the true rate constant can be increasingly underestimated. This explanation may account for some of the difference between the present and the previous studies (*8*, *9*). The dead-time in the previous studies was longer, about 2.2 ms (*8*), which would have exacerbated this effect as well.

Furthermore, an underestimation of the folding rate constant will produce an apparent burst phase amplitude even when one does not actually exist. The zero time amplitude of the measured phase is calculated based upon the folding rate constant: $A_{observed}(t_0) = A_{observed}(\tau_d)e^{k_f\tau_d}$. An underestimated rate will, upon extrapolation back to t_0, reduced the reported amplitude of the major phase, $A_{observed}(t_0)$, thereby generating an apparent missing amplitude. Therefore, both a burst-phase loss of amplitude and nonlinear chevron behavior can come from a single cause, an underestimation of folding rate constants. They do not necessarily provide independent evidence for the formation of a kinetic intermediate.

Double-Jump Measurements. Given the difficulty of measuring rate constants in a heterogeneous folding mixture, it is desirable to decrease the amplitude of the minor phases. Ubiquitin has three *trans*-prolines, residues whose isomerization in the unfolded state is known to produce a slow-folding population (*8*). We implemented a double-jump (N → U → N) refolding protocol to reduce the proline-related slow phases. The native protein is allowed to unfold at 4.7 M GdmCl for 10 s (about 10 unfolding half-lives). Before the prolines in the native, trans configuration have a chance to isomerize in the denatured state, the concentrated denaturant solution is diluted and folding proceeds. This procedure produces a denatured population that, unlike the single-jump population, contains essentially only the native proline configurations. The result of this protocol is a decrease in the amplitude of the slower phases that also are better resolved from the fastest phase (Figure 2b). The rate constants of the fastest phase measured in this manner are in excellent agreement with those from the single-jump measurements (Figure 3a). There is no indication of a plateau in the refolding rate constant, and the zero-time value of the fluorescence signal does not have a burst-phase loss of amplitude (Figure 3b).

Continuous-Flow Measurements. Given the discrepancy between the present and previous folding studies (*8, 9*), we sought to examine whether instrumental artifacts could exist in our measurements (e.g., inaccurate dead-time measurement or inadequate mixing). We conducted multiple continuous-flow measurements at different flow-speeds to alter the dead-time, or the unobservable portion of the reaction (Figure 4). The fluorescent level is measured for about 20 ms for reactions having aged for times between 1.3 and 11 ms. The values for each continuous-flow measurement represent single time points in the refolding experiment and provide information on the refolding rate constant as well as the fluorescence amplitude. The slope of the natural log of the amplitude change versus τ_d plot is the refolding rate constant. Likewise, the *y*-intercept is the zero-time fluorescence signal.

Measurements are performed at four different denaturant concentrations between 0.5 and 2.1 M GdmCl. These denaturant concentrations are chosen as they span the range where a saturation in rate constants and a burst amplitude were reported (*8, 9*). The refolding rate constants determined from the slope of the plot (Figure 4) agree nearly within statistical error with those obtained in the standard stopped-flow measurements (Table 2). Furthermore, the total fluorescence change (*y*-intercept) is identical for refolding at all four GdmCl concentrations. The self-consistency between these and the conventional stopped-flow measurements eliminates inaccurate dead-time values or mixing artifacts as sources for the discrepancy between the present and previous studies. We believe this comparison between stopped-flow and continuous-flow measurements *conducted under the actual refolding conditions* is one of the most accurate methods to confirm the instrument's calibration, because the dead-volume and flow-speed are corroborated by the highly accurate timing of the A/D board. Most importantly, the measurements are independent demonstrations that refolding rate constants do not plateau and all of

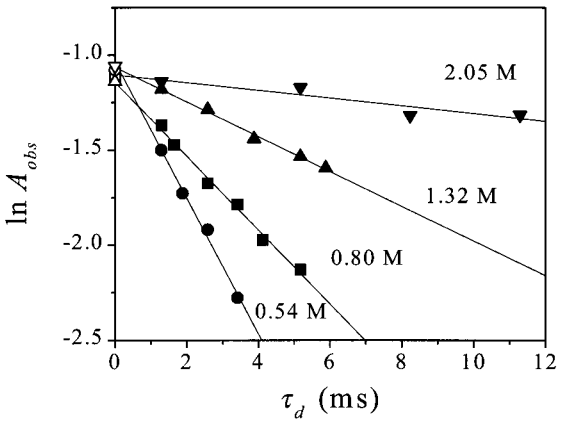

FIGURE 4: Continuous-flow measurements. Continuous-flow values are obtained by varying the flow rate of the peptide and buffer solutions. Because the flow rate is inversely proportional to the dead-time (τ_d) of the instrument, differently aged protein refolding solutions can be produced as indicated by the time axis. The four denaturant conditions, 0.54 M (●), 0.80 M (■), 1.32 M (▲), and 2.05 M (▼), are chosen to test for the presence of a burst phase as well as to demonstrate that the instrument's flow speed is calibrated. The common intercept indicates that all of the change in the raw fluorescence signal, A_{obs}, is accounted for in the observed phase regardless of denaturant concentration, and no submillisecond process occurs in the instrumental dead-time. Open symbols at $\tau_d = 0$ represent the natural logarithm of the voltage change determined from standard stopped-flow measurements with a 1.3 ms dead-time for 0.54 M (○), 0.80 M (□), 1.32 M (△), and 2.05 M (▽). A comparison of the amplitude change and the rate constants (i.e., the slope) to traditional stopped-flow measurements is presented in Table 2.

Table 2: Stopped- and Continuous-Flow Measurements

[GdmCl] (M)	stopped-flow rate constant[a] (s^{-1})	continuous-flow rate constant[b] (s^{-1})	stopped-flow amplitude[a] (V)	continuous-flow amplitude[b] (V)
0.54	368 ± 15	356 ± 19	0.34 ± 0.03	0.36 ± 0.05
0.80	213 ± 2	194 ± 9	0.31 ± 0.02	0.32 ± 0.03
1.32	107 ± 1	92 ± 8	0.32 ± 0.01	0.35 ± 0.04
2.05	16.2 ± 0.5	20.3 ± 4	0.35 ± 0.01	0.33 ± 0.03

[a] Single-jump refolding traces with a 1.3 ms dead-time. [b] From the slope and *y*-intercept of the plot in Figure 4.

the fluorescence signal is accounted for in the observed phases.

Stabilizing Additives. Previous measurements indicated that the presence of 0.4 M sodium sulfate increases the stability of the proposed kinetic intermediate (*9*). Folding rate constants at 25 °C in the presence of 0.4 M sodium sulfate, however, are at the measurement limit of our apparatus, and we would not be able to confidently distinguish between two- and three-state folding models. Hence, we have measured folding in the presence of a lower level of sulfate, 0.23 M, where a potential deviation from two-state behavior would be readily observable. To increase the accuracy of these measurements, they are conducted in the double-jump mode.

The presence of sodium sulfate results in a rightward translation of the chevron (Figure 3a) with the folding and unfolding activation energies changing by about 1 and −0.5 kcal/mol, respectively. As in the absence of additives, all of the fluorescence signal is fully accounted for in the observed phases (Figure 3b), and no roll-over in rate constants is observed despite a potential 1 kcal/mol stabilization of a intermediate.

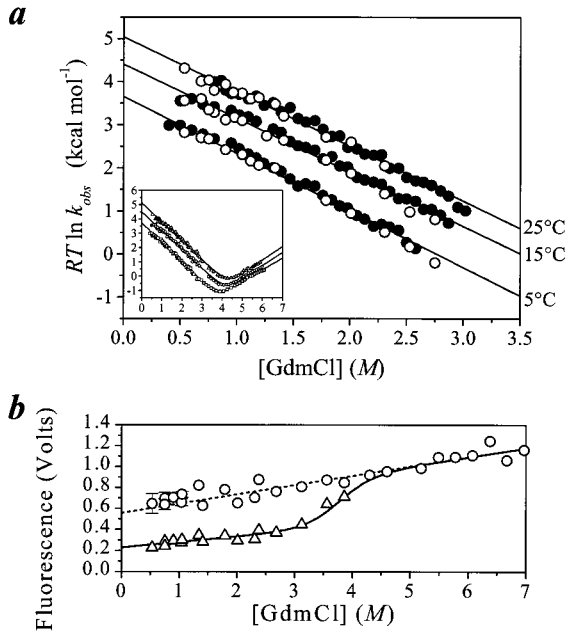

FIGURE 5: Folding in the presence of a stabilizing additive, 1 M sodium chloride, at pH 4.5. (a) Folding activation energy for single-jump (●) and double-jump (○) measurements at 5, 15, and 25 °C. Inset: corresponding refolding activation energy versus GdmCl chevron plots. (b) Fluorescence amplitudes at 25 °C are defined by the raw fluorescence signals at the beginning (○) after extrapolation to $t = 0$ and end (△) of each refolding kinetic measurement. The solid line is a fit to the equilibrium denaturation profile using values from Table 1. The dashed line is the denaturant-dependent baseline of the unfolded state.

Sodium sulfate is commonly employed as a protein precipitate and can lead to aggregation. Because our studies and previous studies (*9*) revealed an additional slow phase in the presence of sulfate, we sought an alternative stabilizing additive. Work by Makhatadze and co-workers indicated that the many types of anions stabilize ubiquitin (*17*). We chose 1.0 M sodium chloride, because chloride ions are already present in the GdmCl buffer. While not as stabilizing as sodium sulfate ($\Delta\Delta G = 1.8$ versus 1.3 kcal M^{-1}), sodium chloride largely reduced the sulfate-dependent slow phase. In the high-salt condition, folding rate constants do not plateau, and all the fluorescence signal is accounted for in the observed phase (Figure 5). As with the previous measurements, a two-state model is adequate to describe Ub folding, even in the presence of stabilizing additives.

DISCUSSION

The role of kinetic intermediates in protein folding remains controversial. Unsettled issues include whether intermediates are required. Do they accelerate or decelerate folding? Are they signatures of a distinct pathway, or adventitious traps in a funnel-like landscape? One of the most fundamental issues is whether stable intermediates accumulate during the folding reaction. One should appreciate that the failure to observe intermediates, as is the case for two-state folding conditions, does not preclude their existence. Two-state folding behavior only requires that any intermediate more stable than the denatured state must be located on the native side of the rate-limiting barrier. Folding may still follow a pathway.

For example, we have proposed that for small globular proteins, folding is a nucleation process with a relatively early

rate-limiting step (*5*, *6*) [see also references (*2*−*4*)]. In this model, folding is limited by diffusive chain motions through solution with multiple transient collisions in a search for a topologically, but not necessarily structurally, nativelike transition state. Beyond the transition state, exposed chain loops condense onto the core, forming the detailed nativelike elements such as secondary structures, possibly through a series of distinct, stable intermediates. This is observed for the folding of cyt *c* (*18*). These post-transition-state intermediates are still important in guiding folding even though they do not accumulate during a refolding experiment.

Given the strong constraint two-state folding behavior places on possible folding models, it is important to establish when folding deviates from a two-state model. The most frequently applied method to establish two-state behavior is the "chevron analysis." When all the standard free energy and surface area burial are accounted for in the observed single-exponential reaction, a burst-phase intermediate cannot exist which is stable relative to the denatured state and buries a significant amount of surface area.

Conversely, when a protein folds through a stable intermediate, a decrease in the denaturant dependence of refolding rate constants is observed (Figure 1b) (*9*). Such "roll-over" behavior is seen in medium-sized proteins such as RNase H where the formation of a specific intermediate is confirmed by a variety of other methods including HX pulse labeling (*19*), mutation (*20*), and native-state HX (*21*). In some other systems, however, such roll-over behavior is attributed to protein aggregation (*22*), movement of the transition state toward the unfolded state (*23*), or inadequate pH control upon buffer dilution (unpublished results). Some other burst-phase signals may be due to the denatured polypeptide responding to the new, poorer solvent conditions rather than to formation of a distinct folding intermediate (*6*, *24*−*26*), although other interpretations have been proposed (*27*−*29*).

Ub is a model protein for which conflicting data exist regarding whether it folds via a stable kinetic intermediate. In the present studies, we did not detect the previously observed signatures for such a species, either a plateau in refolding rate constants or a burst-phase loss of signal (*8*, *9*). Our observation is seen both in the presence and in the absence of stabilizing additives and in single-jump, double-jump, and continuous-flow modes. In conjunction with previous HX pulse labeling (*7*, *8*, *11*) and stopped-flow circular dichroism studies (*11*) that failed to observe H-bond and secondary structure formation in the first few milliseconds of folding, we conclude that a two-state folding model is adequate to describe Ub folding. Just as importantly, these studies stress that additional experimental tests, including measurements of the protection from HX and the application of double-jump techniques, are extremely useful in establishing when folding rate constants deviate from two-state behavior and a folding intermediate truly exists.

It is exciting to speculate on the results of NMR EX1/EX2 HX methods advanced by Robertson and co-workers (*30*) which can measure extremely fast folding rate constants, $>1000\ s^{-1}$, in the absence of denaturants. These methods are near-perfect double-jump measurements, because unfolding is followed by rapid refolding, and proline residues are unable to isomerize appreciably. We believe these measurements can further examine the applicability of the two-state model for Ub folding.

ACKNOWLEDGMENT

We thank N. Kallenbach, S. W. Englander, A. Robertson, K. Meisner, S. Berry, A. Fernandez, Kevin Shi, and T. Pan for numerous enlightening discussions and comments on the manuscript, and X. Fang for suggesting the continuous-flow measurements. A ubiquitin expression vector was generously provided by K. D. Wilkinson.

REFERENCES

1. Jackson, S. E. (1998) *Folding Des. 3*, R81−91.
2. Abkevich, V. I., Gutin, A. M., and Shakhnovich, E. I. (1994) *Biochemistry 33*, 10026−10036.
3. Fersht, A. R. (1995) *Proc. Natl. Acad. Sci. U.S.A. 92*, 10869−10873.
4. Thirumalai, D., and Guo, Z. (1995) *Biopolymers 35*, 137−140.
5. Sosnick, T. R., Mayne, L., Hiller, R., and Englander, S. W. (1995) in *Peptide and Protein Folding Workshop* (DeGrado, W. F., Ed.) pp 52−80, International Business Communications, Philadelphia, PA.
6. Sosnick, T. R., Mayne, L., and Englander, S. W. (1996) *Proteins: Struct., Funct., Genet. 24*, 413−426.
7. Briggs, M. S., and Roder, H. (1992) *Proc. Natl. Acad. Sci. U.S.A. 89*, 2017−2021.
8. Khorasanizadeh, S., Peters, I. D., Butt, T. R., and Roder, H. (1993) *Biochemistry 32*, 7054−7063.
9. Khorasanizadeh, S., Peters, I. D., and Roder, H. (1996) *Nat. Struct. Biol. 3*, 193−205.
10. Matthews, C. R. (1987) *Methods Enzymol. 154*, 498−511.
11. Gladwin, S. T., and Evans, P. A. (1996) *Folding Des. 1*, 407−417.
12. Krantz, B. A., Moran, L. B., Kentsis, A., and Sosnick, T. R. (2000) *Nat. Struct. Biol. 7*, 62−71.
13. Sabelko, J., Ervin, J., and Gruebele, M. (1999) *Proc. Natl. Acad. Sci. U.S.A. 96*, 6031−6036.
14. Larsen, C. N., Krantz, B. A., and Wilkinson, K. D. (1998) *Biochemistry 37*, 3358−3368.
15. Jackson, S. E., and Fersht, A. R. (1991) *Biochemistry 30*, 10436−10443.
16. Grantcharova, V. P., and Baker, D. (1997) *Biochemistry 36*, 15685−15692.
17. Makhatadze, G. I., Lopez, M. M., Richardson, J. M., III, and Thomas, S. T. (1998) *Protein Sci. 7*, 689−697.
18. Bai, Y., Sosnick, T. R., Mayne, L., and Englander, S. W. (1995) *Science 269*, 192−197.
19. Raschke, T. M., and Marqusee, S. (1997) *Nat. Struct. Biol. 4*, 298−304.
20. Raschke, T. M., Kho, J., and Marqusee, S. (1999) *Nat. Struct. Biol. 6*, 825−831.
21. Chamberlain, A. K., Handel, T. M., and Marqusee, S. (1996) *Nat. Struct. Biol. 3*, 782−787.
22. Silow, M., Tan, Y. J., Fersht, A. R., and Oliveberg, M. (1999) *Biochemistry 38*, 13006−13012.
23. Otzen, D. E., Kristensen, O., Proctor, M., and Oliveberg, M. (1999) *Biochemistry 38*, 6499−6511.
24. Chan, C.-K., Hu, Y., Takahashi, S., Rousseau, D. L., Eaton, W. A., and Hofrichter, J. (1997) *Proc. Natl. Acad. Sci. U.S.A. 94*, 1779−1784.
25. Sosnick, T. R., Shtilerman, M. D., Mayne, L., and Englander, S. W. (1997) *Proc. Natl. Acad. Sci. U.S.A. 94*, 8545−8550.
26. Qi, P. X., Sosnick, T. R., and Englander, S. W. (1998) *Nat. Struct. Biol. 5*, 882−884.
27. Shastry, M. C., and Roder, H. (1998) *Nat. Struct. Biol. 5*, 385−392.
28. Hagen, S. J., and Eaton, W. A. (2000) *J. Mol. Biol. 297*, 781−789.
29. Akiyama, S., Takahashi, S., Ishimori, K., and Morishima, I. (2000) *Nat. Struct. Biol. 7*, 514−520.
30. Arrington, C. B., and Robertson, A. D. (1997) *Biochemistry 36*, 8686−8691.

BI000792+